Thermal Coefficients and Thermal Conductivities of Solid and Liquid Phases for Pure Ag, Pure Sn and Their Binary Alloys

Fatma Meydaneri[1] and Buket Saatçi[1*]

[1] Department of Physics, Faculty of Arts and Sciences, Erciyes University, 38039, Kayseri, Turkey.
Fax: +90 352 437 49 33 Phone: +90 352 437 49 01 / 33 122 meydaneri@yahoo.com, bayender@erciyes.edu.tr

Abstract - The variations of thermal conductivities of solid phases versus temperature for pure Sn and eutectic Sn-3.5 wt. % Ag, Sn- 1.5 wt. % Ag binary alloys were measured with a radial heat flow apparatus. The thermal conductivities of the solid phases at their melting temperature were also found to be 0.606 ± 0.06, 0.84 ± 0.09, 0.69 ± 0.07 W/K.cm. From the graphs of the solid phases thermal conductivity variations versus temperature, temperature coefficients for pure Sn, pure Ag and eutectic Sn-3.5 wt. % Ag, Sn- 1.5 wt. % Ag binary alloys were found to be 0.00098, 0.00024, 0.00087, 0.0014 K^{-1}, respectively. The thermal conductivity ratios of liquid phase to solid phase for the pure Sn and eutectic Sn-3.5 wt. % Ag binary alloy at their melting temperature were found to be 1.11 and 1.09 with a Bridgman type directional solidification apparatus. Thus the thermal conductivities of liquid phases for pure Sn and eutectic Sn-3.5 wt. % Ag binary alloy at their melting temperature were evaluated to be 0.67 and 0.92 W/K.cm, respectively by using the values of solid phase thermal conductivities, κ_S and the thermal conductivity ratios of liquid phase to solid phase, R.

Keyword: Thermal Conductivity, Radial Heat Flow, Directional Solidification, Ag-Sn Alloy, Thermal Coefficient.

1. Introduction

Recently, Sn-based alloys have been investigated intensively as potential alternative anode materials for lithium ion batteries because of its higher capacity storage than that of the carbonaceous anodes. Lowering the melting temperature of solder has been shown to be one of the key factors required for achieving lead-free electronics packaging. Lead-tin alloys have been used as soldering materials for a long time. However, lead is a heavy poisonous metal and can be harmful to human health. The European Union (EU) has promulgated directives, such as WEEE and RoHS, on 1 July 2006, to restrict the use of Pb in electronic products. Thus, there is an urgent demand for lead-free solders in the electronic industry. A low processing temperature is desirable for preventing heat damage to electronic devices during soldering, and this is a reason for the adoption of other low melting temperature alloys, i.e., Sn-Ag binary alloy and Ag-Sn ternary alloys [1-24]. The lead-tin alloy systems have been the most commonly used soldering materials in electronic interconnection and packaging because of their low cost and unique combination of physical, chemical, mechanical properties, manufacturability and reliability. During soldering, the molten solders may react with substrates resulting in the formation of intermetalic compounds (IMC)(s) at the interface. It is well known that IMC(s) at the interface have significant effect on the performance of joints. Therefore, information on interfacial reaction between solder and substrate is fundamentally important for the reliability evaluation of electronic joints. Among these Sn-based alloys, Sn-Ag alloy is one of the most promising candidates for Pb-free solder [25-28]. There are many studies dedicated to the study of mechanical properties of lead-free solder materials, including tensile properties, better ductility, higher strength superior resistance to creep and thermal fatigue, under different conditions [29-37].

At high temperature, the microstructure of Sn-base solders would significantly change, and consequently their mechanical properties would be affected. Knowledge about the phase diagram and the thermo-dynamic properties of the studied alloy is required to predict the thermal behaviour, the microstructure evolution of the solder itself and the possible interfacial reactions between solder and substrate [5].

For pure Ag, pure Sn and their binary alloys do not satisfy some technologic parameters as working temperature, for example. The knowledge of the thermodynamics of materials provide fundamental information about the stability of phases and about the driving forces for chemical reactions and diffusion processes. Hence, the purpose of this study is to determine thermal coefficients and thermal conductivities of solid and liquid phases in order to estimated of some thermodynamic properties such as electrical resistivity ρ, Gibbs-Thomson coefficient (Γ), solid-liquid interfacial energy (σ_{SL}) and grain boundary energy (σ_{GB}). These data are of great importance for the development of electronic materials, interconnection technologies, sliding properties, especially in microelectronics and modern industry. Further, these thermal conductivity values will help to people doing the measurement and modeling of these kinds of thermophysical properties.

The thermal conductivity, κ, is one of the main fundamental properties of materials such as density, melting point, entropy, resistance, and crystal structure parameters and it plays a critical role in controlling the performance and

stability of materials. Thermal properties of materials are very important in many industrial applications. The investigation of thermal conductivity is a valuable tool for the study of transport mechanisms of alloys. Although the value of κ for pure materials was obtained theoretically and experimentally, there are not enough information and data available about the thermal conductivity of alloys. The values of κ for alloys change, as in pure materials, not only with temperature but also it changes by compositions of the materials. In the experimental determination of the thermal conductivity of solids, a number of different methods of measurements are required for different ranges of temperature and for various classes of materials having different ranges of thermal conductivity values. A particular method may thus be preferable over the others for a given material and temperature range, and no one method is suitable for all the required conditions of measurement. The various methods for the measurement of thermal conductivity fall in two categories: the steady state and none steady state methods. In the steady state methods of measurement, the specimen is subjected to a temperature profile that is time invariant, and the thermal conductivity is determined directly by measuring the rate of heat flow per unit area and temperature gradient after equilibrium has been reached. In the none steady state methods, the temperature distribution in the specimen varies with time, and the measurement of the rate of temperature change, which normally determines the thermal diffusivity, replaces the measurement of the rate of heat flow. The thermal conductivity is then calculated from the thermal diffusivity with a further knowledge of the density and specific heat of the material

Many attempts have been made to determine the thermal conductivity values of solid and liquid phases in various materials by using different methods [38-53]. One of the common techniques for measuring the thermal conductivity of solids is the radial heat flow method. There are several different types of apparatus all employing radial heat flow. The classification is mainly based upon specimen geometry; i.e. cylindrical, spherical, ellipsoidal, concentric sphere, concentric cylinder, and plate methods**.** In present work was used the radial heat flow method. Because, the cylindrical radial heat flow method uses a specimen in the form of a right circular cylinder with a coaxial central hole, that contains either a heater or a heat sink, depending on whether the described heat flow direction is to be radially outward or inward [38]. Temperatures within the specimen are measured by thermocouples. This method was first used for measuring the thermal conductivity of solids for pure materials by Callendar and Nicolson [39] then this method was used by Niven [40] and Powell [41]. A review of radial heat flow methods was presented by McElroy and Moore [42] and this method was widely used for measuring the thermal conductivity of solids for various materials [43-53].

Firstly, the phase diagram of Ag-Sn binary alloy is given in Figure 1 [54]. Then, the dependence of thermal conductivity of solid phases on temperature for the pure Sn and eutectic Sn-3.5 wt. % Ag, Sn- 1.5 wt. % Ag binary alloys has been investigated. Secondly, the temperature coefficients of the pure Sn, pure Ag and their binary alloys have been determined from the graph of the thermal conductivity versus temperature. Finally, the thermal conductivity ratios of liquid phases to solid phases at their melting temperatures have been determined to obtain the thermal conductivities of liquid phases for the pure Sn and eutectic Sn-3.5 wt. % Ag, Sn- 1.5 wt. % Ag binary alloys.

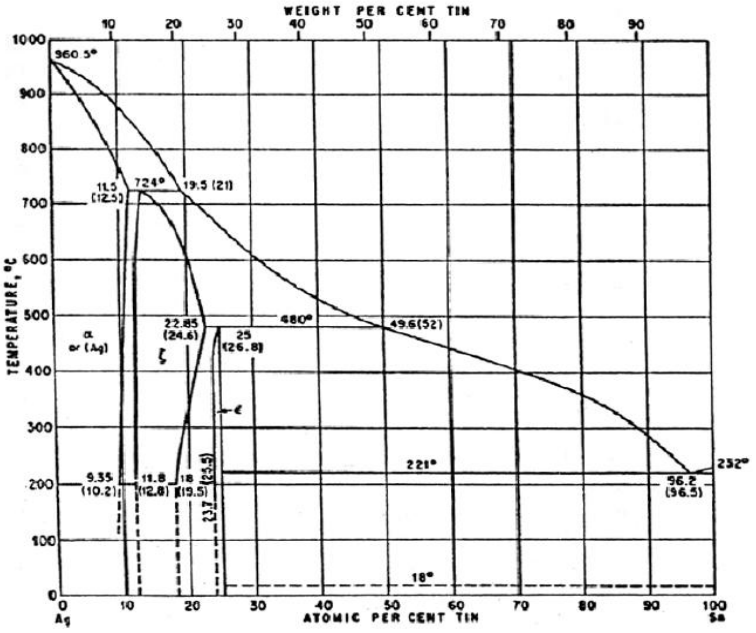

Fig. 1. The phase diagram of Ag-Sn binary alloy [54].

2. Experimental Procedure

2.1. Measurement of thermal conductivity of solid phases

In present work, the radial heat flow apparatus was chosen to determine the thermal conductivity of solids, because of its symmetrical characteristics. A radial heat flow apparatus, originally designed by Gündüz and Hunt [43, 44] and modified by Maraşlı and Hunt [45] were used to experimentally determine the thermal conductivity of solid phases. More details of the apparatus are described in reference [43-53], as shown Figure 2. The radial heat flow apparatus consists of a central heating element and a water cooling jacket. The central heating element was a 1.7 mm Kanthal A-1 wire inside a thin walled alumina tube (3 mm OD x 2 mm ID x 120 mm long) and was used to heat specimen from center. The water cooling jacket is made of stainless steel and was used to cool the outside of the specimen. To get radial heat flow, the specimen was heated from the centre and the outside of the specimen was kept cool with the water cooling jacket. The temperature gradient on the specimen could be changed by placing different materials into the gap between the specimen and the water cooling jacket.

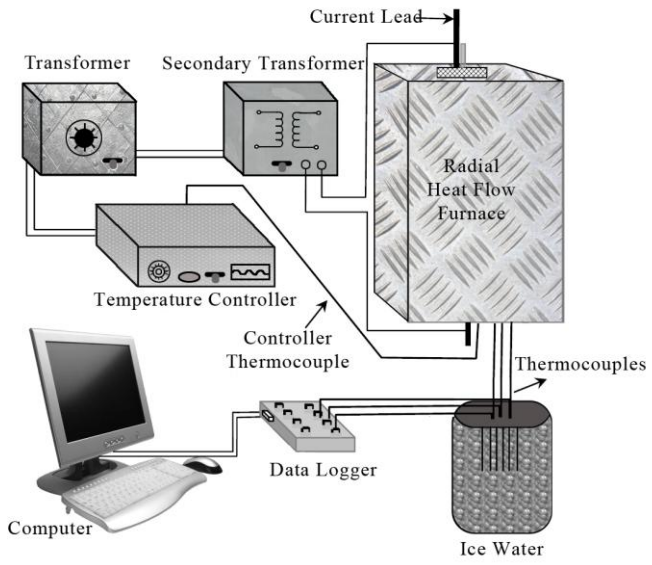

Fig. 2. Block diagram of radial heat flow system.

Consider a cylindrical specimen heated by a heating element along the axis at the center of the specimen. At the steady-state conditions, The radial temperature gradient in the cylindrical specimen is given by Fourier's law

$$G_S = \left(\frac{dT}{dr}\right) = -\frac{Q}{A\kappa_S} \qquad (1)$$

where Q is the total input power from the centre of the specimen, A is the surface area of the specimen and κ_S is the thermal conductivity of the solid phase. Integration of the Equation (1) gives

$$\kappa_S = a_0 \frac{Q}{T_1 - T_2} \qquad (2)$$

where $a_0 = \ln(r_2 - r_1)/2\pi\ell$ is an experimental constant, l is the length of the heating element, r_1 and r_2 are fixed distances from the centre of the sample, and T_1 and T_2 are temperatures at the fixed positions ($r_1 > r_2$) r_1 and r_2, respectively.

$$\kappa_S = \frac{Q\ln(r_2/r_1)}{2\pi\ell(T_1 - T_2)} \qquad (3)$$

Equation (3) could be used to obtain the thermal conductivity of the solid phase by measuring the difference in temperature between the two fixed points for a given power level provided that the vertical temperature variation is minimum or zero [53]. If the value of Q, r_1, r_2, ℓ, T_1 and T_2 can be accurately measured for the well-characterized sample, then reliable κ_S values can be obtained [48].

The crucible was made from high purity graphite obtained from *Morganite* as symmetrical as possible to ensure that the isotherms were almost parallel to the central axis, as shown in Figure 3. (b). The crucible consisted of three parts, a 120 mm length of cylindrical tube, the top and the bottom lids. The lids were pushed tightly into the cylindrical tube. The cylindrical tube was 30 mm ID x 40 mm OD x 120 mm long. The top and bottom lids were made as symmetrical as possible. The top lid had four air or feeding holes, one vertical thermocouple hole and one central hole for the alumina tube. The bottom lid had five holes, three holes for the fixed thermocouples (one of them for the control unit, two others for measurement thermocouples), one for the vertical thermocouple and one for the central alumina tube, as shown in Figure 3. (c). The control unit thermocouple and one of the measurement thermocouples were placed 2-3 mm away form the central alumina tube, the control and the measurement thermocouple holes were drilled at 85.5^0 to the ends of the cylinder tube. The vertical (moveable) and one of the measurements thermocouple holes were drilled 12-15 mm away from the centre, as shown in Figure 3. (a).

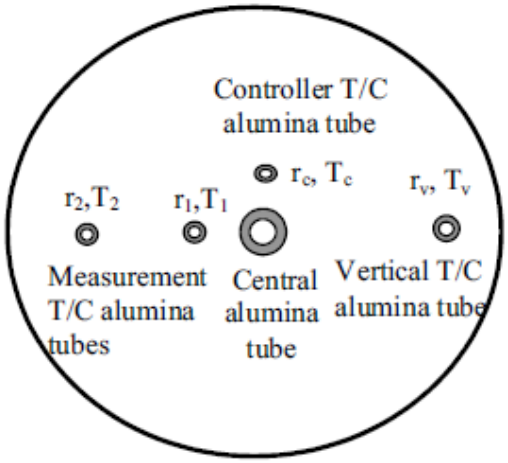

(a)

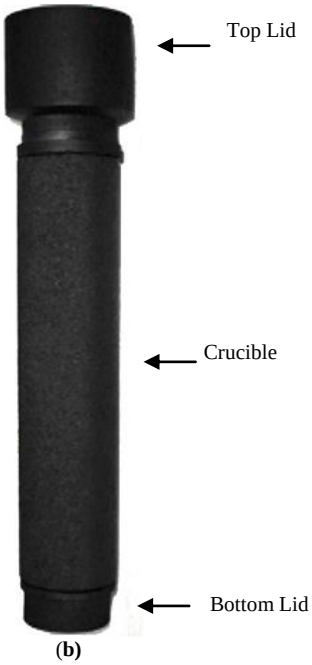

(b)

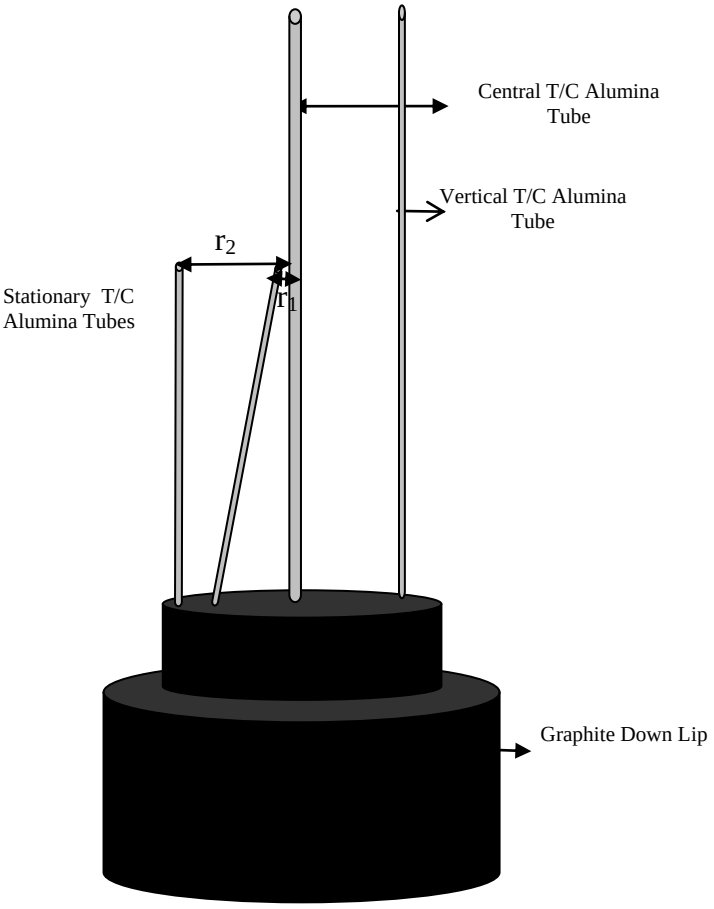

(c)

Fig. 3. (a). Transverse section of the sample. (**b).** Graphite crucible. **(c).** Longitudinal section of a part of the sample at the central of the specimen.

Sufficient amount of materials to produce an ingot of approximately 120 mm long and 30 mm in diameter were melted in a graphite crucible using the vacuum melting furnace by using 99.9 % pure Sn and 99.9 % pure Ag supplied by *Alfa Aesar*. The specific amount of metal was melted under the vacuum approximately 50 ^{0}C above the melting point of the alloys. Then it was stirred with a graphite plunger. After that, the molten metal was poured into the graphite crucible held in a specially constructed casting furnace at approximately 50 ^{0}C above the melting temperature of the alloys. It was then directionally solidified from the bottom to the top to ensure that the crucible was completely filled. The sample was then taken out from the casting furnace and placed into the radial heat flow apparatus.

The specimen was heated from the center using a single heating wire in steps of of 20-50 ^{0}C up to 10 ^{0}C below the melting temperature and the outside of the specimen was kept cool with the water cooling jacket to get a radial temperature gradient. The length of the central heating wire was chosen to be slightly longer than the length of the specimen to make the vertical isotherms parallel to the axis. The gap between the cooling jacket and the specimen was filled with free running sand to get a large radial temperature gradient on the specimen. The larger radial temperature gradient is desired to increase the experimental sensitivity for the solid phase thermal conductivity measurements. The temperature of the specimen was controlled with a Euroterm *9706* type controller and the temperature in the specimen was stable to ± 0.01-0.02 ^{0}C for at least 2 hours. At the steady state, the total input power and the temperatures of the stationary thermocouples were recorded with *Hewlett Packard 34401* type multimeters and *Pico TC-08* model data logger. The vertical isotherm for each setting was made parallel to the axis at the measurement region by moving the central heater up and down, as shown in Figure 4. After all the desired power setting and the temperature measurements had been completed during the heating procedure, the specimen was started in same steps cool to the room temperature.

Then the sample was moved from the furnace and cut transversely near the temperature measurement point, after that the specimen was ground and polished for the measurements of the r_1 and r_2. The positions of the thermocouples were then photographed with digital camera placed in conjunction with an Olympus BH2 optical microscope and a graticule (100 × 0.01 = 1 mm) was also photographed using the same objective. The photographs of the positions of the thermocouples and the graticule were superimposed on one another using *Adobe PhotoShop CS2* version software so that accurate measurement of the distances of stationary thermocouples could be made to an accuracy of ± 10 μm. The transverse and longitudinal sections of the specimen were examined for the porosity, crack and casting defects to make sure that these would not introduce any errors to the measurements.

Experimental data for the thermal conductivity determination of solid phases for pure Sn and eutectic Sn-3.5 wt. % Ag, Sn- 1.5 wt. % Ag binary alloys are given in Table 1, Table 2, Table 3. The variations of solid phase thermal conductivity versus temperature for pure Sn, pure Ag [56] and eutectic Sn-3.5 wt. % Ag, Sn- 1.5 wt. % Ag binary alloys are also shown in Figure 5.

2.2. Determination of the temperature coefficient

For a given composition, the dependence of the thermal conductivity of solid phase on temperature can be expressed as [57]

$$\kappa_S = \kappa_{S0}\left[1+\alpha(T-T_0)\right] \qquad (4)$$

where κ_S is the thermal conductivity of the solid phase at the temperature T, κ_{S0} is the thermal conductivity at the initial temperature and α is the temperature coefficient. From Equation (4), the temperature coefficient, α is written as

$$\alpha = \frac{\kappa_S - \kappa_{S0}}{\kappa_{S0}(T-T_0)} = \frac{1}{\kappa_{S0}}\frac{\Delta\kappa}{\Delta T} \qquad (5)$$

This means that the temperature coefficient, α can be obtained from the graph of thermal conductivity versus temperature. The values used in the determination of the temperature coefficient, α of solid phases are given in Table 4.

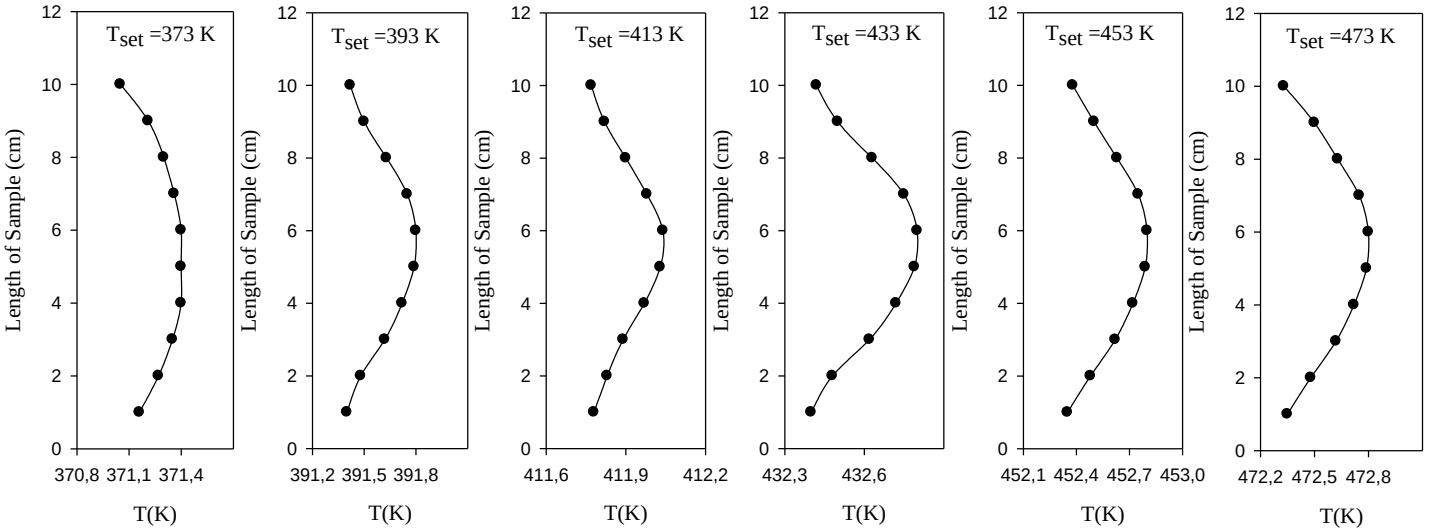

Fig. 4. Typical vertical temperature variations in the specimen at different setting temperatures for Sn.

Table 1. Experimental data for the thermal conductivity determination of solid pure Sn.

T (K)	Q (W)	T_1 (K)	T_2 (K)	$\Delta T=T_1-T_2$ (K)	κ_S (W/K.cm)
373	17.79	371.70	371.25	0.45	0.672
393	23.78	392.41	391.79	0.62	0.652
413	27.22	412.69	411.96	0.73	0.633
433	31,26	432.31	431.45	0.86	0.617
453	38.65	452.88	451.83	1.05	0.625
473	42.79	473.13	471.93	1.2	0.606

r_1= 0.247 cm. r_2 = 1.361 cm. l =15.5 cm. a_0 = 0.017cm^{-1}

Table 2. Experimental data for the thermal conductivity determination of solid Sn-3.5 wt. % Ag alloy.

T (K)	Q (W)	T_1 (K)	T_2 (K)	ΔT (K)	κ_S (W/K.cm)
323	42.95	323.80	323.32	0.48	0.98
343	47.17	343.59	343.06	0.53	0.97
363	48.37	363.63	363.08	0.55	0.96
383	51.50	383.90	383.29	0.61	0.92
403	57.85	404.04	403.34	0.70	0.90
423	78.59	424.10	423.14	0.96	0.90
443	107.62	444.15	442.83	1.32	0.89
463	132.61	464.86	463.20	1.66	0.87
483	149.97	485.49	483.54	1.95	0.84

r_1= 0.462 cm. r_2 = 1.524 cm. l =16.4 cm. a_0 = 0.011 cm^{-1}

Table 3. Experimental data for the thermal conductivity determination of solid Sn-1.5 wt. % Ag alloy.

T(K)	Q(W)	T_1 (K)	T_2 (K)	ΔT(K)	κ_s (W/K.cm)
323	9.43	323.69	323.49	0.20	0.89
343	15.90	343.57	343.22	0.35	0.86
363	26.49	364.06	363.46	0.60	0.83
383	32.69	383.98	383.23	0.75	0.82
403	41.73	404.38	403.36	1.02	0.77
423	55.15	423.51	422.12	1.39	0.75
443	64.50	443.78	442.10	1.68	0.72
463	75.92	464.83	462.77	2.06	0.70
483	90.14	486.35	483.88	2.47	0.69

r_1= 0.239 cm. r_2 = 1.565 cm. l =15.5 cm. a_0 = 0.019 cm^{-1}

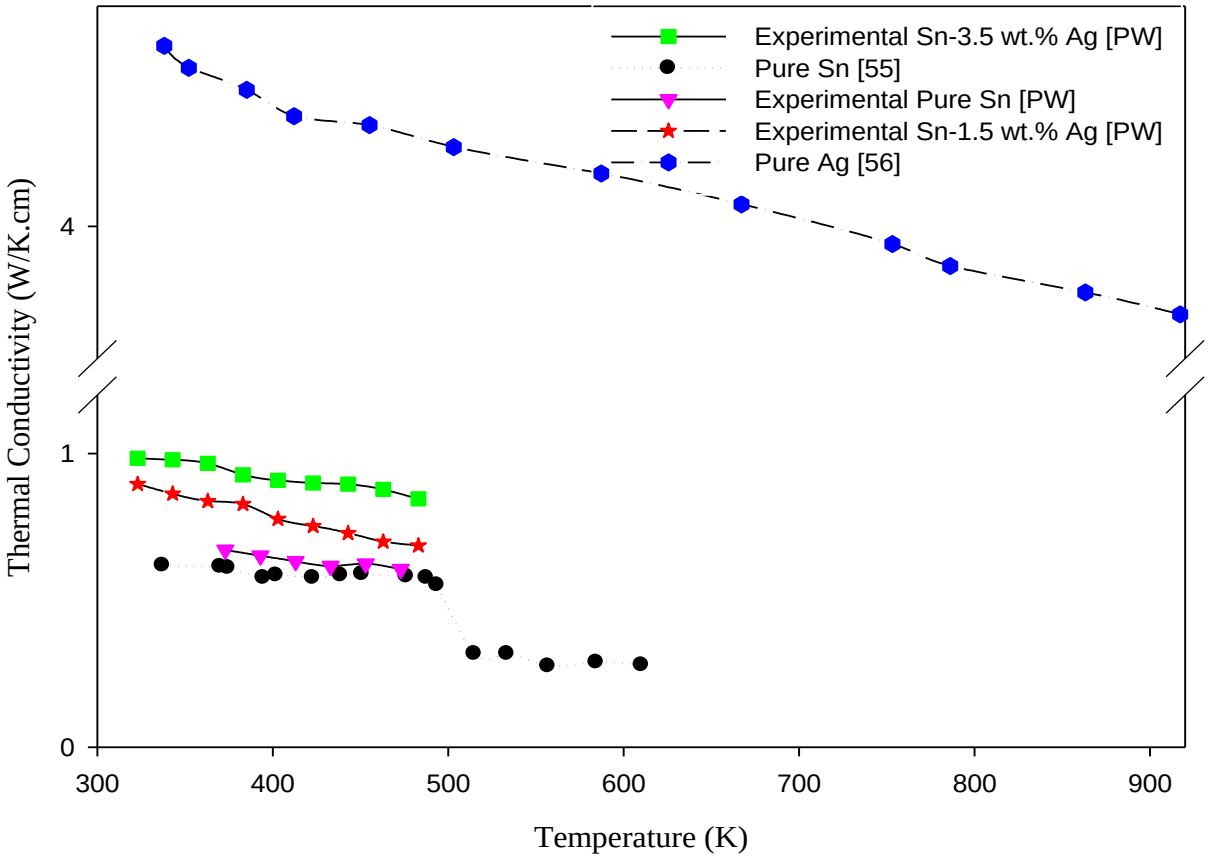

Fig. 5. Thermal conductivities of pure Sn [55], pure Ag [56] and Sn- 3.5 wt. % Ag, Sn- 1.5 wt. % Ag binary alloys versus temperature.

Table 4. Temperature coefficient (α) obtained from the graph of thermal conductivity versus temperature.

System	κ_{s0} (W/K.cm)	κ_s (W/K.cm)	T_0 (K)	T (K)	α (K^{-1})
Pure Sn	0.672	0.606	373	473	0.00098
Pure Ag	4.41	3.80	338.2	917.2	0.00024
Sn- 3.5 wt. % Ag	0.984	0.846	323	483	0.00087
Sn-1.5 wt. % Ag	0.896	0.687	323	483	0.0014

2.3. Thermal conductivity ratio of liquid phase to solid phase

It is not possible to measure the thermal conductivity of liquid phase with the radial heat flow apparatus since a thick liquid layer (10 mm) is required. A layer of this size would certainly have led to convection. If the ratio of thermal conductivity of the liquid phase to solid phase is known and the thermal conductivity of the solid phase is measured at the melting temperature, the thermal conductivity of the liquid phase can then be evaluated. The thermal conductivity ratio can be obtained during directional growth with the Bridgman type growth apparatus. The heat flow away from the interface through the solid phase must balance that liquid phase plus the latent heat generated at the interface, i.e. [58]

$$VL = \kappa_S G_S - \kappa_L G_L \qquad (6)$$

where V is the growth rate, L is the latent heat, G_S and G_L are the temperature gradients in the solid and liquid, respectively and κ_S and κ_L are the thermal conductivities of the solid and the liquid phases, respectively. For very low growth rates $VL \ll \kappa_S G_S - \kappa_L G_L$, so that the conductivity ratio, R is given by

$$\kappa_S G_S \cong \kappa_L G_L, \qquad R = \frac{\kappa_L}{\kappa_S} = \frac{G_S}{G_L} \qquad (7)$$

If the right hand side of Equation (7) is obtained and the value of κ_S is measured, then the liquid thermal conductivity can be evaluated from Equation (7) [43-53].

In the present work, the thermal conductivity ratio of liquid phase to solid phase, R, was obtained in a directional growth apparatus (Bridgman type) [59]. A directional growth apparatus which was first constructed by McCartney [60] was used to determine the thermal conductivity ratio $R=\kappa_S/\kappa_L$. A thin walled graphite crucible was produced by drilling out a graphite rod of 6.35 mm outer diameter and 220 mm total length to a depth of 180 mm with a 4 mm inner diameter. As mentioned above, the sufficient amount of materials (pure Sn and Ag-Sn binary alloys) was melted in a vacuum furnace. After stirring, the molten metal was poured into thin walled graphite crucibles and the molten alloy was then directionally frozen from bottom to top to ensure that the crucible was completely full. Then, the sample was positioned in a Bridgeman type furnace in a graphite rod of 6.35 mm outer diameter and 220 mm total length to a depth of 180 mm with a 4 mm inner diameter and it was heated to 50 ^{0}C over the melting temperature. The specimen was then left to reach the thermal equilibrium for at least two hours. The temperature in the specimen was measured with an insulated 0.5 mm K type thermocouple. 1.2 mm OD x 0.8 mm ID alumina tube was used to insulate the thermocouple from the melt and the thermocouple was placed perpendicular to heat flow (growth direction). The temperature on the sample was controlled to an accuracy of ± 0.5 K with a *Eurotherm 815 S* type controller and the temperature of fluid in the reservoir was approximately 15-20 ^{0}C. When the specimen temperature stabilized, the directional growth was begun by turning on the motor and the temperature change with time was recorded by a *Pico TC-08* type data logger via computer. When the solid-liquid interface passed the thermocouple, a change in the slope of the temperature change with time was observed. In the present measurements, the growth rate was 5 mm/minute. After the temperature reading is 20-30 K below the melting temperature the growth was stopped and the samples were quenched by rapidly pulling it down into the fluid reservoir.

The conductivity ratio was evaluated from the change in the slope of the temperature versus time curves. From the temperature versus time curves, the slope of the liquid and solid phases can be written as

$$\left(\frac{dT}{dt}\right)_L = \left(\frac{dT}{dx}\right)_L \left(\frac{dx}{dt}\right)_L = G_L V \qquad (8)$$

and

$$\left(\frac{dT}{dt}\right)_S = \left(\frac{dT}{dx}\right)_S \left(\frac{dx}{dt}\right)_S = G_S V \qquad (9)$$

From Equations (7), (8) and (9) the thermal conductivity ratio can be written as

$$R = \frac{\kappa_L}{\kappa_S} = \frac{G_S}{G_L} = \frac{\left(\frac{dT}{dt}\right)_S}{\left(\frac{dT}{dt}\right)_L} \qquad (10)$$

where the values of $\left(\frac{dT}{dt}\right)_S$ and $\left(\frac{dT}{dt}\right)_L$ for pure Sn and eutectic Sn- 3.5 wt. % Ag alloy were directly measured from the temperature versus time curve as shown in Figure 6 and Figure 7, respectively.

3. Results and Discussions

3.1. Thermal conductivity and temperature coefficient of solid phase

The thermal conductivities of the κ_S versus temperature for pure Sn, pure Ag [56] and eutectic Sn- 3.5 wt. % Ag, Sn-1.5 wt. % Ag binary alloys are shown in Figure 5. The thermal conductivities of solid phases for pure Sn, pure Ag and eutectic Sn- 3.5 wt. % Ag, Sn-1.5 wt. % Ag binary alloys decreases with increasing temperature and the values of κ_S for eutectic Sn- 3.5 wt. % Ag, Sn-1.5 wt. % Ag binary alloys lie between the values of κ_S for pure Ag and pure Sn as shown in Figure 5.

The estimated experimental error in the measurement of κ_S is the sum of the fractional uncertainty of the measurements of power, temperature difference, length of heating wire and thermocouples positions which can be expressed as

$$\left|\frac{\Delta\kappa_S}{\kappa_S}\right| = \left|\frac{\Delta Q}{Q}\right| + \left|\frac{\Delta T^*}{\Delta T}\right| + \left|\frac{\Delta \ell}{\ell}\right| + \left|\frac{\Delta r_1}{r_1 \ln r_2/r_1}\right| + \left|\frac{\Delta r_2}{r_2 \ln r_2/r_1}\right| \qquad (11)$$

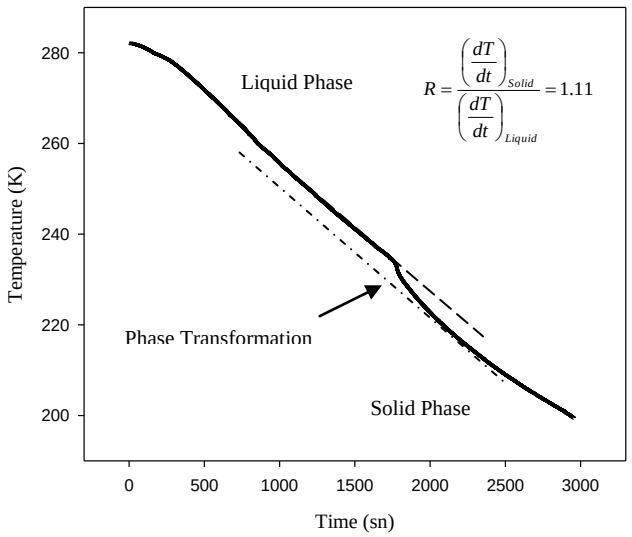

Fig. 6. Temperature versus time for pure Sn.

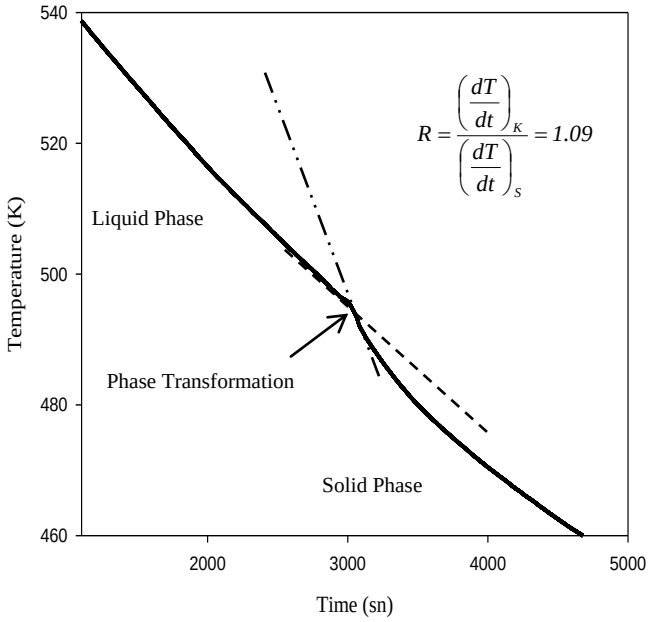

Fig. 7. Cooling rate of Sn- 3.5 wt. % Ag eutectic binary alloy.

3.1.1. Fractional uncertainty in the power measurement

The input power is expressed as

$$Q = V_h I \tag{12}$$

where V_h is the potential difference between the ends of the central heating wire and I is the current outgoing from the central heating wire. The fractional uncertainty in the power measurement can be expressed as

$$\left|\frac{\Delta Q}{Q}\right| = \left|\frac{\Delta V_h}{V_h}\right| + \left|\frac{\Delta I}{I}\right| \tag{13}$$

The potential difference between the ends of the central heating wire was measured with a *Hewlett-Packard 34401-A* multimeter to accuracy of ± 1 %. Current outgoing from the central heating wire was measured with *Clampmeter* to accuracy of ± 1 %. Thus the total fractional uncertainty in power measurement is about 2 %.

3.1.2. The fractional uncertainty in the measurement of heating wire's length, ℓ, and the fixed distances (r_1, r_2)

As can be seen from Tables 1-3, the average lengths of heating wire was 155 mm and measured with an accuracy of ± 0.5 mm. The fractional uncertainty in the measurement of heating wire's length is about 0.3 %. The fixed distances of thermocouples from centre of the specimen (r_1, r_2) were measured using *Adobe PhotoShop CS2* version software from the photographs of the thermocouple's positions to an accuracy of ± 10 μm. The fixed distances from the center of specimen are about 2-4 mm and 13-15 mm. The fractional uncertainty in the measurements of the fixed distances is between 0.2 % and 0.5 %. Therefore the total fractional uncertainty for measuring the heating wire's length and the fixed distances is 1 %.

3.1.3. Fractional uncertainty in the measurement of temperature difference between two thermocouples, $\Delta T = T_1 - T_2$ at the setting temperature

The temperatures on the specimen were measured by using K type thermocouples. The difference of the thermocouples readings, ΔT* at the same point of specimen with a setting temperature must be known or measured to determine the uncertainty of temperature measurement. To determine the difference of thermocouples readings, the thermocouples were calibrated by detecting the melting point of metalic material as shown in Figure 8. It can be seen from Figure 9 the difference of thermocouples readings, ΔT*, at the melting temperature of metalic material was ± 0.1-0.2 K. As can be seen for Ag-Sn binary alloys from Tables 2-3, the temperature difference between two fixed thermocouples, $\Delta T = T_1 - T_2$ at 483 K changes between 1.95 K and 2.47 K. Thus the uncertainty in the temperature measurement at 483 K is about 9 %.

Therefore the total fractional uncertainty in the measurements of thermal conductivity of solid phases is about 12 %.

The thermal conductivities of solid phases for pure Sn and eutectic Sn- 3.5 wt. % Ag, Sn-1.5 wt. % Ag binary alloys at approximately their melting temperature are found to be 0.606 ± 0.07, 0.84 ± 0.10, 0.69 ± 0.08 W/K.cm, respectively. In addition, the temperature coefficients for pure Sn, pure Ag and eutectic Sn- 3.5 wt. % Ag, Sn-1.5 wt. % Ag binary alloys

were found to be 0.00098, 0.00024, 0.00087, 0.0014 K^{-1}, respectively from Figure 5.

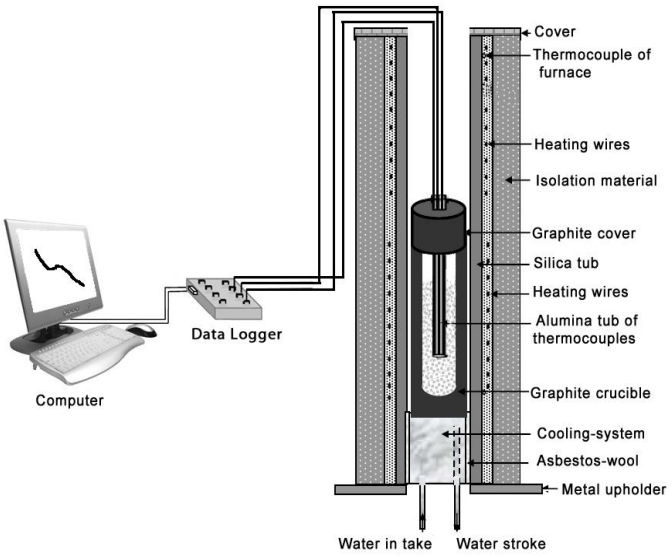

Fig. 8. Schematic-drawing of calibration experimental setup.

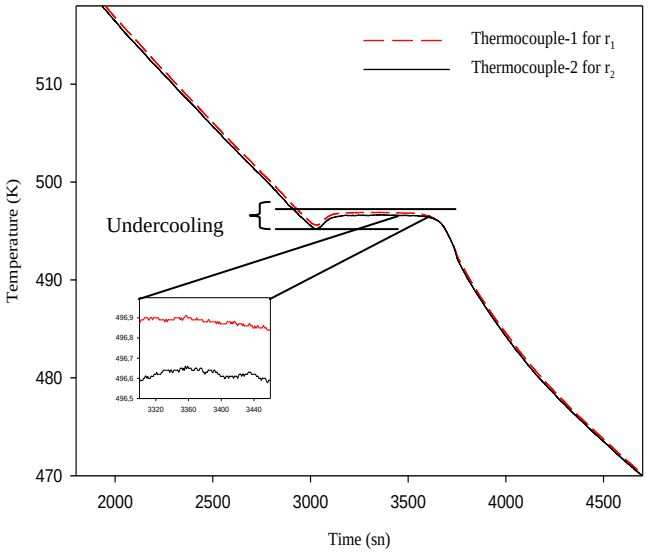

Fig. 9. Thermocouples calibration by detecting melting temperature.

3.2. Thermal conductivity ratio of liquid phase to solid phase

As can be seen from Figure 6 and Figure 7 the value of R can be evaluated from the ratio of the solid phase cooling rate to the liquid phase cooling rate. The values of R for pure Sn and eutectic Sn- 3.5 wt. % Ag alloy at their melting temperatures were found to be 1.11 and 1.09, respectively by Bridgman type directional solidification apparatus and the results are given in the Table 5. The thermal conductivities of solid phases for the same metalic materials at their melting temperature are measured to be 0.606 ± 0.07, 0.84 ± 0.10, 0.69 ± 0.08 W/K.cm, respectively with radial heat flow apparatus. Thus the thermal conductivities of liquid phases, κ_L for pure Sn and eutectic Sn- 3.5 wt. % Ag alloy at their melting temperature were determined to be 0.67 and 0.92 W/K.cm, respectively from Equation (10) using the values of κ_S and R and the evaluated values are also given in Table 5.

The value of R for Sn- 1.5 wt. % Ag alloy at its melting temperature was found from $R = \kappa_L$ *(eutectic liquid)* / κ_S *(solid).* κ_L (eutectic liquid) was found to be 0.92 W/K.cm. The thermal conductivity of solid phase for Sn- 3.5 wt. % Ag alloy at approximately its melting temperature was found to be 0.69 ± 0.08 W/K.cm with radial heat flow apparatus. Thus, the value of R for same binary alloy at its melting temperature was found to be 1.33. The values of thermal conductivities used in the calculations and a comparison of our results with values of κ_S found in the literature is also given in Table 5. As can bee seen from Table 5 and Figure 5, the values measured in present work for pure Sn and Ag-Sn binary alloys are in a good agreement with the values obtained by Touloukian [55, 56, 61, 62]. In the literature, there are very little datas for Ag-Sn binary alloys to make comparison but the values of κ_S for above Ag-Sn binary alloys are between the κ_S values of pure Sn and pure Ag measured in present work.

4. Conclusions

Thermal conductivities of solid and liquid phases for pure Sn and Sn- 3.5 wt. % Ag, Sn- 1.5 wt. % Ag binary alloys were measured as functions of temperature. The results are summarized as follows:

a) The variations of thermal conductivities of solid phase versus temperature for pure Sn and Sn- 3.5 wt. % Ag, Sn- 1.5 wt. % Ag binary alloys have been measured with ± 12 % experimental error by using radial heat flow apparatus.

b) The thermal conductivities of solid phases at approximately their melting temperature and the temperature coefficients for the pure Sn, the pure Ag and Sn- 3.5 wt. % Ag, Sn- 1.5 wt. % Ag binary alloys have been determined from the graphs of the solid phase thermal conductivity versus temperature.

c) The thermal conductivity ratios of liquid phase to solid phase for pure Sn and Sn- 3.5 wt. % Ag alloy at their melting temperature have been determined with a Bridgeman type directional solidification apparatus.

d) The value of R for Sn- 1.5 wt. % Ag binary alloy at its melting temperature was found from

$R = \kappa_L$ *(eutectic liquid)* / κ_S *(solid).*

e) The thermal conductivity of liquid phases for pure Sn and eutectic Sn- 3.5 wt. % Ag alloy at their melting temperatures have been evaluated by using the values of solid phase thermal conductivities and the thermal conductivity ratios of liquid phase to solid phase.

5. Acknowledgments

This project was supported by Erciyes University Scientific Research Project Unit under Contract No: FBD-09-846. Authors would like to thank to Erciyes University Scientific

Research Project Unit for their financial supports. The authors would like to thank to Mehmet Özdemir for experimental studies help.

Table 5. Thermal conductivities of solid and liquid phase for pure Sn, pure Ag and Sn- 3.5 wt. % Ag, Sn- 1.5 wt. % Ag, binary alloys.

System	Phase	Temperature (K)	κ (W/K.cm) [PW]	κ (W/K.cm) [Literature]	$R=\kappa_L/\kappa_S$
Pure Sn	Liquid Sn Solid Sn	504 473	0.672 0.606	- 0.602[56]	1.11
Pure Ag	Liquid Ag Solid Ag	1234 917.2	- -	3.55[61] 3.80[57]	-
Sn- 3.5 wt. % Ag (Eutectic Composition)	(Liquid Phase) Sn- 3.5 wt. % Ag (Solid Phase) Sn- 3.5 wt. % Ag	494 483	0.92 0.84	0.611[62]	1.06
Sn- 1.5 wt. % Ag	(Liquid Phase) Sn- 1.5 wt. % Ag (Solid Phase) Sn- 1.5 wt. % Ag	494 483	0.92 0.69	- 0.603[62]	1.33

[PW]: Present Work

6. References

[1] Chiapyng Lee, Chung-Yung Lin, Yee-Wen Yen, The 260 ˚C phase equilibria of the Sn-Sb-Ag ternary system and interfacial reactions at the Sn-Sb/Ag joints, Journal of Alloys and Compounds,458, 436-445, (2008).

[2] A. Rae, A. Handwerker, NEMI's Lead-Free Alloy, Circuits Assembly, 2004, pp. 20-25.

[3] K.J. Puttlitz, K.A. Stalter, Handbook of Lead-Free Solder Technology for Microelectronic Assemblies, Marcel Dekker, New York, 2004, pp. 239-300.

[4] C.-H.Wang, S.-W. Chen, Acta Mater., 54, (1), (2006), 247-253.

[5] S. Hassama, Z. Baharib, B. Legendre, Phase diagram of the Ag-Bi-Sb ternary system, Journal of Alloys and Compounds, 315, (2001), 211-217,

[6] Suganuma K, Niihara K. J Mater Res, 1998;13:2859.

[7] Ohtani H, Miyashita M, Ishida K. J Jpn Inst Met, 1999;63:685.

[8] Suganuma K, Murata T, Noguchi H, Toyoda Y. J Mater Res, 2000;15:884.

[9] Vassilev GP, Tedenac JC, Dobrev ES, Evtimova SK. Arch Metal, 2001;46:249.

[10] Vassilev GP, Evtimova SK, Tedenac JC, Dobrev ES. J Alloys Compd, 2002;334:182.

[11] Date M, Shoji T, Fujiyoshi M, Sato K, Tu KN. Scripta Mater, 2004;51:641.

[12] Kim KS, Yang JM, Yu CH, Jung IO, Kim HH. J Alloys Compd, 2004;379:314.

[13] Song JM, Liu PC, Shih CL, Lin KL. J Electron Mater, 2005;34:1249.

[14] Yu DQ, Xie HP, Wang L. J Alloys Compd, 2004;385:119.

[15] Lin KL, Liu PC, Song JM. In: Proceedings of the 2004 electronic components and technology conference IEEE; 2004. p. 1310.

[16] Chou CY, Chen SW. Acta Mater, 2006;54:2393.

[17] Dragan Manasijevi´c , Jan V˘re˘st´al , Du˘sko Mini´c , Ale˘s Kroupa , Dragana ˘ Zivkovi´c, ˘Zivan ˘ Zivkovi´c, Phase equilibria and thermodynamics of the Bi-Sb-Sn ternary system, Journal of Alloys and Compounds, 438, (2007), 150-157.

[18] J. Sigelko, S. Choi, K.N. Subramanian, J.P. Lucas, T.R. Bieler, J. Electron. Mater., 28, (1999), 1184.

[19] Ab Tew M, Selvaduray G. lead-free solders in microelectronics [J]. Mater Sci Eng R, 2000, R27: 95-141.

[20] Zeng K, K.N. Tu. Six cases of reliability study of Pb-free solder joints in electronic packaging technology [J]. Mater Sci Eng R, 2002, R38: 55 - 105.

[21] C. M. L. Wu, Yu DQ, Law CMT, et al. Properties of lead-free solder alloys with rare earth element additions [J]. Mater Sci Eng R, 2004, R44: 1- 44.

[22] Kim KS, Imanishi T, Suganuma K, Kumamoto S, Aihara M. Effects of composition on microstructure and on thermal stability of Sn-Ag- In lead-free soldered joints. Trans MRS-J, 2004; 29 (5): 2005 - 8.

[23] Vianco PT, Rejent JA. Properties of ternary Sn-Ag-Bi solder alloys: Part II-Wettability and mechanical properties analyses. J Electron Mater 1999; 28(10):1138-43.

[24] Artaki I, Jackson AM, Vianco PT. Evaluation of lead-free solder joints in electronic assemblies. J Electron Mater 1994; 23(8):757-64.

[25] Y. Chonan, T. Komiyama, J. Onuki, R. Urao, T. Kimura, T. Nagano, Mater. Trans., 43, (2002), 1887-1890.

[26] C.M. Chuang, P.C. Shih, K.L. Lin, J. Electron. Mater., 33, (2004), 1-6.

[27] S.L. Allen, M.R. Notis, R.R. Chromik, R.P. Vinci, J. Mater. Res., 19, (2004), 1425-1431.

[28] J.Y. Tsai, Y.C. Hu, C.M. Tsai, C.R. Kao, J. Electron. Mater., 32, (2003), 1203-1208.

[29] J. Wang, L.G. Zhang, H.S. Liu, L.B. Liu, Z.P. Jin, Interfacial reaction between Sn-Ag alloys and Ni substrate, Journal of Alloys and Compounds, 455, (2008), 159-163.

[30] J. Liang, N. Gollhardt, P.S. Lee, S.A. Schroeder,W.L. Morris, Fatigue Fract. Eng. M, 19, (1996), 1401.

[31] P.T. Vianco, J.A. Rejent, A.C. Kilgo, J. Electron. Mater., 33, (2004), 1373-1380.

[32] M. Kerr, N. Chawla, Acta Mater., 52, (2004), 4527.

[33] J. Liang, S. Downes, N. Dariavach,D. Shangguan, S.M. Heinrich, J. Electron. Mater., 33, (2004), 1507.

[34] J. Liang, N. Dariavach, G. Barr, Z. Fang, J. Electron. Mater., 35, (2006), 372.

[35] M.L. Huang, L.Wang, C.M.L.Wu, J. Mater. Res., 17, (2002), 2897.
[36] M. Amagai, M. Watanabe, M. Omiya, K. Kishimoto, T. Shibuya, Microelectron. Reliab., 42, (2002), 951.
[37] Sun-Kyoung Seo a, Sung K. Kang b, Da-Yuan Shih b, Hyuck Mo Lee, The evolution of microstructure and microhardness of Sn-Ag and Sn-Cu solders during high temperature aging, Microelectronics Reliability, 49, (2009), 288-295.
[38] Y.S.Touloukian, R.W.Powell, C.Y.Ho and P.G.Klemens, Thermal Conductivity, Metallic Elements and Alloys, Thermophysical Properties of Matter, Vol. 1, (New York: Plenum) pp. 3a-25a, 1970.
[39] H.L.Callender and J.T.Nicolson, Brt. Assoc. Adv. Sci. Rept. Ann. Meeting, 418, (1897)22.
[40] C.Niven, Proc. Roy.Soc.A 76, (1905) 34.
[41] R.W.Powell, Proc. Phys. Soc. 51, (1939) 407.
[42] D.L.McElroy and J.P. Moore, In Thermal Conductivity, Vol. 1, Chapter 4, Academic Press, London, pp.185, 1969.
[43] M.Gündüz and J. D. Hunt, Acta Mat, 33, (1985) 1651.
[44] M.Gündüz and J.D. Hunt, Acta Mat, 37, (1989)1839.
[45] N.Maraşlı and J.D. Hunt, Acta Mat., 44, (1996) 1085.
[46] B.Saatçi and H. Pamuk, J. of Physics: Condens. Mater, 18, (2006) 10143.
[47] B. Saatçi, M. Arı, M. Gündüz, F. Meydaneri, M. Bozoklu and S. Durmuş, J. of Physics: Condens Mater, 18, (2006) 10643.
[48] Saatçi B, Maraşlı N and Gündüz M, 2007 Thermochimica Acta 454 128-34.
[49] Erol M, Keşlioğlu K, Şahingöz R, Maraşlı N. Experimental determination of thermal conductivity of solid and liquid phases in Bi–Sn and Zn–Mg binary eutectic alloys. Metals Miner Int 2005;11:421.
[50] Saatçi, B., Çimen, S., Pamuk, H. and Gündüz**,** M.**,** The interfacial free energy of solid Sn on the boundary interface with liquid Cd–Sn eutectic solution, 19, 326219 (11pp), 2007.
[51] Meydaneri F, Saatçi B, Gündüz M, Özdemir M. Measurement of solid–liquid interfacial energy for solid Zn in the Zn–Cd eutectic system. Surf Sci 2007;601:2171.
[52] Kaygısız, Y, Ocak, Y., Akbulut, S., Keşlioğlu, K., Maraşlı, N., Çadırlı, E., Kaya, H., Thermal conductivity and interfacial energies of solid Sn in the Sn-Cu Alloy s Journal of Material Science 2009.
[53] Akbulut, S., Ocak, Y., Maraşlı, N., Keşlioğlu, K., Kaya, H.,Çadırlı, E., Determination of solid–liquid interfacial energies in the In–Bi–Sn ternary alloy, J. Phys. D: Appl. Phys., 41, (2008), 175302, (10pp).
[54] Hansen M and Anderko K 1985 Constitutions of Binary Alloys 2nd edition (New York: McGraw-Hill) p. 919.
[55] **[55]** Touloukian YS, Powell RW, Ho CY, Klemens PG. Thermal conductivity metallic elements and alloys, vol. 1. Washington: New York; 1970. p. 404.
[56] Touloukian YS, Powell RW, Ho CY, Klemens PG. Thermal conductivity metallic elements and alloys, vol. 1. Washington: New York; 1970. p. 346.
[57] S. Akbulut, Y. Ocak, K. Keşlioğlu and N. Maraşlı, Thermal conductivities of solid and liquid phases for Neopentylglycol, Aminomethylpropanediol and their binary alloy, Journal of Physics and Chemistry of Solids, (2008).
[58] D.A. Porter and K.E. Easterling, Phase Transformations in Metals and Alloys, Van Nostrnad Reinhold Co. Ltd., UK, pp.204, 1991.
[59] E.Çadırlı, D.Phil. Thesis, Erciyes University, Turkey, 1997 pp. 77.
[60] D.G. Mc Cartney, D.Phil. Thesis, , University of Oxford, UK, pp. 85-175, 1981.
[61] Touloukian YS, Powell RW, Ho CY, Klemens PG. Thermal conductivity metallic elements and alloys, vol. 1. Washington: New York; 1970. p. 348.
[62] Touloukian YS, Powell RW, Ho CY, Klemens PG. Thermal conductivity, metallic elements and alloys, vol. 1. Washington: New York; 1970. (Thermal conductivity of Tin+ Silver Alloys) p. 845.